



## Effect of annealing treatment on morphologies and gas sensing properties of ZnO nanorods

Jian-jiao ZHANG, Er-jun GUO, Li-ping WANG, Hong-yan YUE, Guo-jian CAO, Liang SONG

College of Materials Science and Engineering, Harbin University of Science and Technology, Harbin 150040, China

Received 3 February 2013; accepted 5 July 2013

**Abstract:** The high-temperature stabilization of ZnO nanorods synthesized by hydrothermal treatment was investigated. The structure and morphologies of ZnO nanorods were characterized by XRD and SEM, respectively. The thermal stability of ZnO nanorods was also detected by thermal gravity analyzing. Thermal annealing treatment results indicate that ZnO nanorods are fundamentally stable when annealing temperature is lower than 600 °C. When annealing temperature is beyond 600 °C, the diameters of ZnO nanorods obviously decrease and the aggravating tendency of nanorods between each other also increase. Annealing treatment can greatly influence the gas sensing properties of ZnO nanorods. Comparing with ZnO nanorods without annealing treatment, the gas sensing property of ZnO nanorods to H<sub>2</sub> with concentration of  $2.5 \times 10^{-6}$  can increase from 2.22 to 3.56. ZnO nanorods annealed at 400 °C exhibit optimum gas sensing property to H<sub>2</sub> gas.

**Key words:** ZnO nanorods; annealing treatment; gas sensing property

### 1 Introduction

Nowadays, one-dimensional ZnO nanomaterials have become a hotspot of researchers due to their special properties, such as absorption of UV light, resistance to radiation, luminescence characteristics and piezoelectric properties [1]. Among their diverse morphologies, ZnO nanorods hold an excellent potential in lots of optoelectronic fields, involving UV lasing emission [2], light emission diodes [3], gas sensors [4] and solar cells [5]. Many techniques have been developed to fabricate ZnO nanorods, such as chemical vapor deposition [6], pulse laser deposition [7], radio frequency magnetron sputtering [8], microwave heating [9], sol-gel method [10], hydrothermal growth [11], template-assisted growth [12] and refluxing method [13]. However, it is well known that ZnO nanorods have low crystal quality with lattice defects and surface defects due to low growth temperature [14]. In order to reduce the defects and improve the qualities of ZnO, post-annealing treatment is an effective method to enhance the crystalline and application qualities of ZnO nanorods by decreasing the

oxygen vacancy concentration, deep level defects and surface defect recombination [15].

Several studies have been reported about the annealing process of ZnO nanorods under different ambient atmospheres and their effects on ZnO properties. For instance, WANG et al [16] studied the effect of annealing temperatures on the magnetic properties of as-synthesized Zn<sub>1-x</sub>Mn<sub>x</sub>O nanorods. The result indicated that the coercivity and saturation magnetization increased obviously after annealing treatment. LEE et al [17] studied the effects of annealing at 400 °C for 1 h on the optical properties of ZnO nanorods. The result indicated that the reason for the increase in the ratio of UV to visible emission of ZnO nanorods annealed in oxygen or forming gas was attributed to the reduction in the concentration of the oxygen defects and to the less OH groups on the surface of ZnO nanorod. Moreover, XIANG et al [18] reported that ZnO nanorods embedded Ag nanoparticles exhibited good gas sensing to ethanol gas. However, the reason of morphologies change of ZnO nanorods undergoing post-annealing treatment is not elucidated thoroughly and the correlation of annealing treatment dependence of gas sensing property

**Foundation item:** Project (51201052) supported by the National Natural Science Foundation of China; Project (2012RFQXG107) supported by the Innovative Talent Fund of Harbin City; Project (E201056) supported by Natural Science Foundation of Heilongjiang Province of China; Project (1252G022) supported by the Program for Youth Academic Backbone in Heilongjiang Provincial University, China

**Corresponding author:** Er-jun GUO; Tel: +86-451-86390008; E-mail: [guoerjun@126.com](mailto:guoerjun@126.com)

DOI: 10.1016/S1003-6326(14)63119-8

of ZnO nanorods is seldom evaluated.

Thus, it is necessary to study the stabilization of ZnO nanomaterials in order to fulfill the practical detecting requirement. WAGN et al [19] reported that ZnO nanorods with the diameters ranging from 100 to 200 nm and the length of several micrometers can be properly used in oxygen gas sensing applications. Here, the morphology changing process of ZnO nanorods with similar sizes at different thermal annealing temperatures is studied. The result indicates that the gas sensing property is strong related with annealing treatment and renders the reason for the utilization of ZnO nanorods in gas sensors and other expanding devices.

## 2 Experimental

The starting materials of zinc nitrate, hexamethylenetetramine (HMTA) and sodium hydroxide were purchased from Yaohua Co. Ltd., Tianjin, China. All reagents were analytic a grade. In a typical experimental procedure, 25 mL aqueous solution of zinc nitrate ( $\text{Zn}(\text{NO}_3)_2 \cdot 6\text{H}_2\text{O}$ ) with the concentration of 0.09 mol/L was mixed with isometric solution of HMTA with the concentration of 0.09 mol/L. Then 25 mL aqueous solution of sodium hydroxide (0.9 mol/L) was slowly dropped into the above solution with vigorously magnetic stirring. Afterwards, the mixture solution was ultrasonic irradiated for 30 min with the power of 400 W and transferred into a stainless-steel autoclave with the capacity of 100 mL. The autoclave was then sealed and put into a vacuum drying oven maintained at 100 °C for 24 h. After cooling to room temperature, the white powders were collected and washed for several times with distilled water to remove the impurities and subsequently dried at low temperature of 60 °C. Post-annealing treatment of the obtained precursors was carried out at different temperatures of 400, 600, 800, and 1000 °C for 2 h in muffle furnaces with controlling accuracy of  $\pm 5$  °C.

The crystal structures of the as-synthesized powders were examined by X-ray diffraction (XRD, Philips X'Pert MPD) with Cu  $K_\alpha$  radiation ( $\lambda=0.15406$  nm). The Bragg angle used in the measurement was ranging from 5° to 90° in steps of 0.02 (°)/s. The morphologies and size distributions of the products were further observed by scanning electron microscopy (SEM, FEI-Sirion 200) operating at an acceleration voltage of 20 kV. Thermal analysis was performed by the instrument of TG/DSC STA409 (Netzsch, Germany) with the heating rate of 10 K/min under a nitrogen atmosphere. Thermo-gravimetric analysis was performed by a SHIMADZU TG-20 instrument with the heating rate of 10 K/min under static atmosphere.

The gas sensing properties of ZnO nanorods after annealing treatment were also investigated. The method and instruments of gas sensing test were similar to those reported in Ref. [20]. Firstly, the nanomaterials were dispersed with terpineol and  $\text{H}_2\text{PtCl}_6$  by a slightly grinding in an agate mortar to form a slurry suspension. The mixture suspension was then coated onto the surface of ceramic tubes without covering the electrodes at the terminal part of tubes. Four Au electrodes were connected with the founder of sensor by welding process. A resistance heater was then inserted into the ceramic tubes to render the working temperature of the sensors. The structure illustrator of as-prepared sensor is shown in Fig. 1.

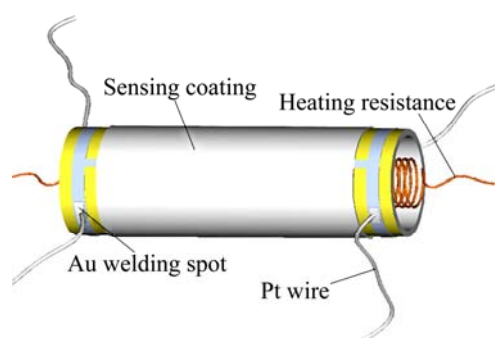


Fig. 1 Structure illustration of side-heating gas sensor

Afterwards, the gained sensor was dried at 100 °C and then put into an oven at the temperature of 450 °C for 2 h to remove the organic. To improve the stability and repeatability, the sensors were aged at 5 V voltages for 10 d in air prior to use. Finally, the gas sensing of ZnO nanomaterials sensor to different gases was carried out and the data of gas sensitivity were recorded by a Labview recording system. The relative response sensitivity ( $S$ ) is defined as  $S=R_a/R_s$ , where  $R_a$  is the resistance in carrier air gas;  $R_s$  is the resistance in the mixture gas of target gas with carrier gas.

## 3 Results and discussion

### 3.1 Effect of annealing temperature on morphology and size of ZnO nanorods

SEM images of ZnO nanorods treated by different annealing temperatures are shown in Fig. 2. It can be seen that the morphologies of ZnO nanorods have no obvious change when annealing temperature is lower than 400 °C. With the increase of temperature, the morphology of ZnO nanorods changes apparently. The diameter of nanorods increases from ~120 nm to ~200 nm and the length becomes shorter from ~1.4 μm to ~0.8 μm. At 800 °C, the diameter of ZnO nanorod increases to ~230 nm, simultaneously, the edges of nanorods become passivation. When the temperature is higher than 1000 °C, the rod-like morphology completely disappears and aggregated particle morphology occurs.

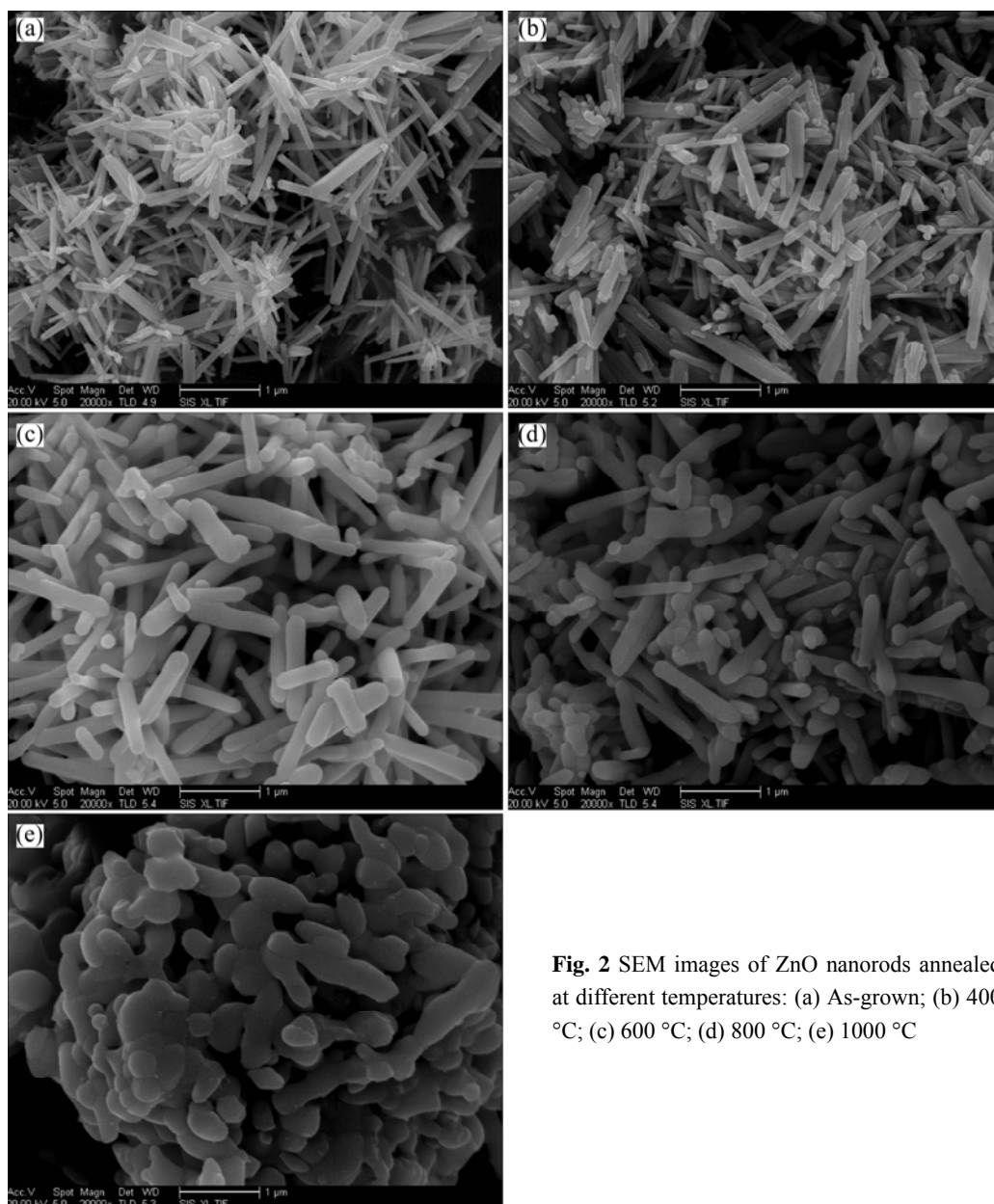


**Fig. 2** SEM images of ZnO nanorods annealed at different temperatures: (a) As-grown; (b) 400 °C; (c) 600 °C; (d) 800 °C; (e) 1000 °C

Figure 3 shows the typical XRD patterns of the as-obtained ZnO nanorods under different annealing temperatures. The diffraction peaks are individually (100), (002), (101), (102), (110), (103) and (112) lattice planes corresponding to the literature (PDF 36-1451). All diffraction peaks can be attributed to wurtzite structured ZnO ( $P6_3mc$ ;  $a=0.3249$  nm,  $c=0.5206$  nm). No other peaks are detected within the detection limit of the XRD instrument. The intense and sharp peaks demonstrate that the as-obtained products are well-crystallized. It can also be found that the diffraction peak height exhibits a descending trend when the products were annealed at 1000 °C.

The thermal gravity (TG) and differential scanning calorimetry (DSC) curves of ZnO nanorods at different annealing temperatures are depicted in Fig. 4.

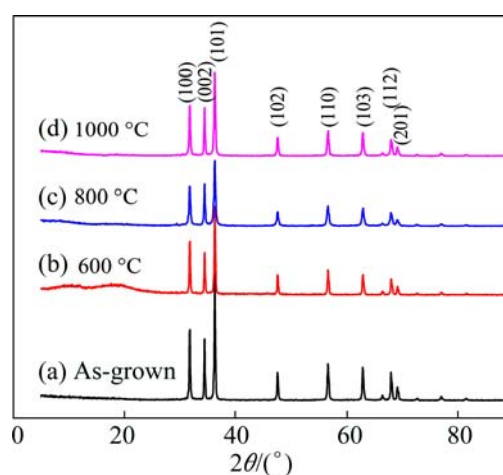


**Fig. 3** XRD patterns of ZnO nanorods annealed at different temperatures

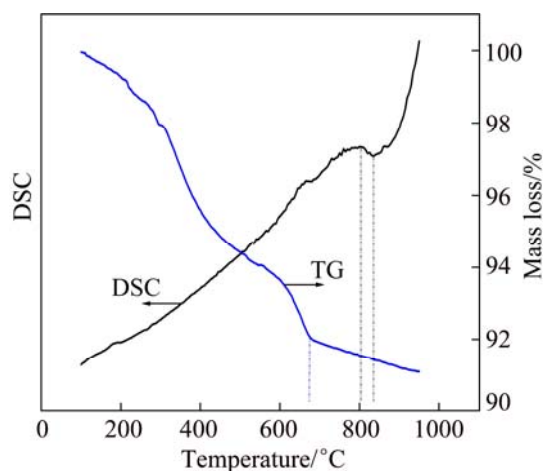


Fig. 4 DSC and TG curves of ZnO nanorods

It can be seen that there is no emergence of absorption or radiate peak in DSC curve when the temperature is lower than 650 °C. But when temperature is over 650 °C, the DSC curve slightly fluctuates. When the temperature is up to 820 °C, the DSC curve begins to descend slightly, which implies the morphology and structure of ZnO nanomaterials change at this point. When the temperature exceeds 900 °C, the curve begins to climb up again. From TG curve, it can be seen that the TG curve continuously descends when the temperature is lower than 670 °C and then slowly descends. It indicates that the mass loss may come from the loss of water and organic substance evaporating from ZnO nanorods.

During the annealing process at high temperature, the microstructures and the stoichiometric ratio of materials will change [21]. Moreover, the migration of grain boundaries of ZnO nanorods is stimulated and the crystalline atom gains more activation energy due to the effect of annealing treatment. In this case, the activated atoms will overcome thermal barrier between crystal grains and freely move to the correct sites in the crystal lattice through diffusion [22]. Hence, the rod-like morphology of ZnO will gradually dissolve and convert to another nanoparticle with round-edge morphology. If the temperature continuously rises up, the grains with lower surface energy will further grow larger, which results in the final nanoparticle with aggregated morphology. Moreover, when the annealing temperature is relative high, the densities of the crystallographic defects, including dislocations, interstitials and vacancies in ZnO nanorods, can also be decreased rapidly [23]. During thermal processing, the highly activated neighboring defective sites between single nanorods will be combined, fractured or broken, finally resulting in the apparent morphological evolution. Considering the above results, the morphology and characteristic of ZnO nanorods will keep stable when the thermal annealing

temperature of ZnO nanorods is lower than 600 °C. In this case, the crystal structure and surface state of ZnO nanorods will be perfectly improved, which renders the reference for subsequent application for gas sensor.

### 3.2 Gas sensing properties of ZnO nanorods

To investigate the effect of annealing treatment on the gas sensing of ZnO nanorods, the curve of gas sensing dependence of annealing temperature is firstly depicted, as shown in Fig. 5.

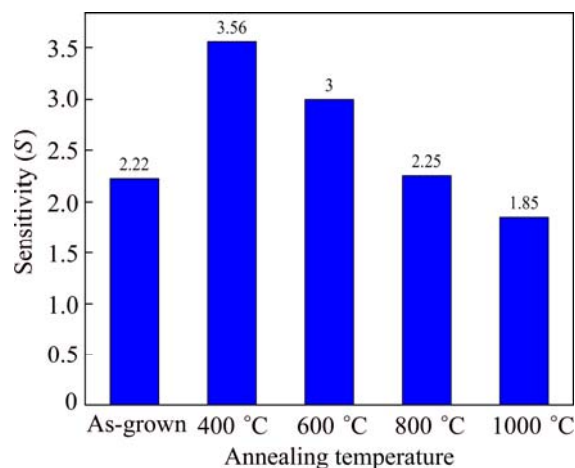


Fig. 5 Gas sensing comparison of ZnO nanorods undergoing different annealing temperatures to  $25 \times 10^{-6}$  H<sub>2</sub> gas

It can be seen that with increasing annealing temperature, ZnO nanorods show a gas sensing discrepancy. The gas sensing value is only 2.25 without annealing treatment. After 400 °C annealing treatment, the gas sensing of ZnO nanorods can reach 3.56. With increasing the temperature from 600 to 1000 °C, the gas sensing decreases from 3 to 1.85.

As mentioned in previous researches, ZnO nanorods directly hydrothermal grown without post-annealing treatment show a large defect concentration and absorption of OH at the surface, which introduces an electron accumulation layer at the surface [24]. In this case, the transfer rate of electron will be limited in the existing layer. It is well known that the size and morphologies determine the properties of ZnO materials. When annealing treatment is initially used, the electron accumulation layer will be reduced for the broken of thermal barrier. In spite that ZnO nanorods maintain previous rod-like appearance, the gas sensing of ZnO nanorods will be significantly improved with increasing temperature. While, with the increasing of annealing temperature up to 600 °C, the atoms of crystals can gain more energy to get across the barrier of grain boundary, so ZnO nanorods exhibit coarse rod-like morphology. In this case, the grain size becomes larger, resulting in the decrease of surface-to-volume ratios of ZnO nanorods. When *n*-type ZnO is exposed to the oxidizing gas, the



position to absorb oxygen molecules will be dramatically reduced. Moreover, during the process of annealing treatment, the oxygen vacancies on the surfaces of ZnO nanorods begin to reduce which are electrically and chemically active [25]. These surface defects also affect the adsorption behaviors of gas molecules on metal oxide surfaces [26], so the gas sensing properties of ZnO nanorods will decline. When annealing temperature rises up to 800 °C, possible oxidation reactions may occur during the annealing treatment. Oxygen atoms will evaporate out of the ZnO lattice, so the  $V_O$ -related defects will be significantly increased, which will lead to the decrease of adsorption sites for gas molecules. In this case, the gas-sensing properties of ZnO nanorods will be further deteriorated. In this experimental condition, 400 °C is the optimum annealing temperature for ZnO nanorods.

According to the above thermal stability results of ZnO nanorods, aging temperature of gas sensor is set near to the optimum annealing temperature of 400 °C. Then, the gas sensing property of ZnO nanorods having experienced thermal treatment at 400 °C is evaluated by selecting  $H_2$  as the target gas. In order to study the effect of operating temperature on the gas sensing value, the concentration of  $H_2$  is maintained as  $25 \times 10^{-6}$ . The curve of sensitivity correlation with different operating temperatures is firstly depicted, as shown in Fig. 6. It can be seen that the sensing value of gas sensor is influenced by the heating temperatures. The sensing value of ZnO sensor firstly increases from 2.22 at 250 °C to 3.56 at 425 °C and then decreases to 2.56 at 490 °C. At 425 °C, the gas sensing can reach maximum value of 3.56. Hence, the operating temperature is finally chosen at 425 °C by adjusting the working voltage of heating resistance near to 5.0 V.

Figure 7 depicts four response curves of nanorods sensors to  $H_2$  gas with different concentrations at 425 °C. At the first stage, the resistance of gas sensor maintains a

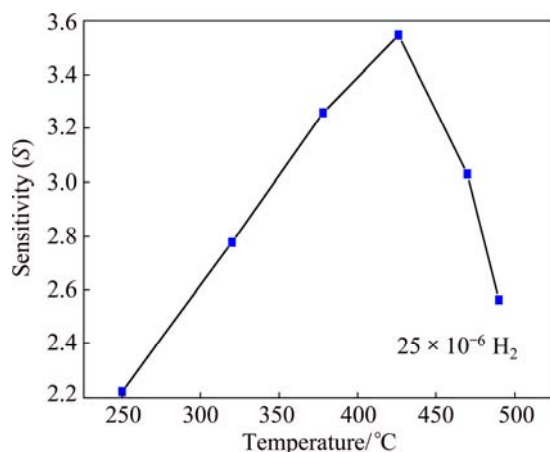


**Fig. 6** Gas sensing of ZnO nanorods to  $H_2$  at different operating temperatures

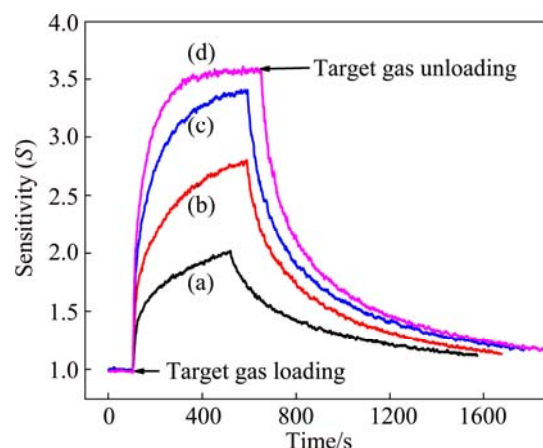


**Fig. 7** Gas sensing of ZnO nanorods to  $H_2$  with different concentrations: (a)  $2.5 \times 10^{-6} H_2$ ; (b)  $5 \times 10^{-6} H_2$ ; (c)  $10 \times 10^{-6} H_2$ ; (d)  $25 \times 10^{-6} H_2$

stable value under the circumstance of continuously introducing the purified air. With the introduction of  $H_2$  gas, all response curves firstly climb up rapidly and then keep up to a stabilized level. Afterwards, when  $H_2$  is unloaded, all the curves begin to decline to the initial platform. It can also be seen that the sensitivity of gas sensor increases with the increase of gas concentration. The gas sensing value is 1.95, 2.63, 3.28 and 3.56 corresponding to  $H_2$  concentration of  $2.5 \times 10^{-6}$ ,  $5 \times 10^{-6}$ ,  $10 \times 10^{-6}$ , and  $25 \times 10^{-6}$ , respectively. But when  $H_2$  concentration increases to  $10 \times 10^{-6}$ , the increase of response sensitivity has no obvious increment, indicating near maximum adsorption of  $H_2$  onto ZnO nanorods sensor. Moreover, with the increase of gas concentration, the response time of ZnO nanorod sensor increases from 15 s at  $2.5 \times 10^{-6}$  to 19 s at  $25 \times 10^{-6}$  and the recover time of ZnO sensor also increases from 1038 s at  $2.5 \times 10^{-6}$  to 1180 s at  $25 \times 10^{-6}$ .

This phenomenon could be explained with the adsorption competition between ambient molecular oxygen and analyte vapors on the surface and the adverse effect of adsorbed analytes on the mobility of free charge carriers [25]. The adsorbates on the surface of ZnO nanorods may function as active scattering centers, thus suppressing the electrical conduction of free carriers, leading to the resistance increase for both oxidizing and reducing analyte exposures. In view of the dynamic detection method differing with condition stationary examination, the results demonstrate that ZnO nanorods after annealing treatment can be reckon as a promising material for fabricating low-cost and high performance gas sensor.

## 4 Conclusions

1) Annealing temperature affects the morphologies

and sizes of ZnO nanorods. With the increase of annealing temperature, the grain size of ZnO nanorod increases progressively. When the temperature is over 800 °C, ZnO nanorods will change into aggregated morphology.

2) The results of DSC and TG analyses indicate that there is a conversion step for ZnO nanorods when annealing temperature gets to 820 °C. At the same time, ZnO nanorods will not maintain initial rod morphology.

3) Annealing treatment can improve the crystal quality and result in enhanced gas sensing properties to H<sub>2</sub>.

## References

- [1] SUN H D, MAKINO T, SEGAWA Y, KAWASAKI M, OHTOMO A, TAMURA K, KOINUMA H. Enhancement of exciton binding energies in ZnO/ZnMgO multiquantum wells [J]. *Journal of Applied Physics*, 2002, 91: 1993–1997.
- [2] ZHANG D K, CHEN S J, DENG Z Q, WANG Y P, LIU Y C, MA D G. Ultraviolet lasing action in ZnO nanosheets [J]. *Journal of Nanoscience and Nanotechnology*, 2010, 10: 6744–6747.
- [3] YANG Q, WANG W, XU S, WANG Z L. Enhancing light emission of ZnO microwire-based diodes by piezo-phototronic effect [J]. *Nano Letters*, 2011, 11: 4012–4017.
- [4] CAROTTA M C, CERVI A, DI NATALE V, GHERARDI S, GIBERTI A, GUIDI V, PUZZOVIO D, VENDEMIATI B, MARTINELLI G, SACERDOTI M. ZnO gas sensors: A comparison between nanoparticles and nanotetrapods-based thick films [J]. *Sensors and Actuators B: Chemical*, 2009, 137: 164–169.
- [5] ZHANG Q, DANDENEAU C S, ZHOU X, CAO G. ZnO nanostructures for dye-sensitized solar cells [J]. *Advanced Materials*, 2009, 21: 4087–4108.
- [6] ZHANG N, YI R, SHI R R, GAO G H, CHEN G, LIU X H. Novel rose-like ZnO nanoflowers synthesized by chemical vapor deposition [J]. *Materials Letters*, 2009, 63: 496–499.
- [7] BABREKAR H A, JEJURIKAR S M, JOG J P, ADHI K P, BHORASKAR S V. Low thermal emissive surface properties of ZnO/polyimide composites prepared by pulsed laser deposition [J]. *Applied Surface Science*, 2011, 257: 1824–1828.
- [8] YANG W F, LIU Z G, PENG D L, ZHANG F, HUANG H L, XIE Y N, WU Z Y. Room-temperature deposition of transparent conducting Al-doped ZnO films by RF magnetron sputtering method [J]. *Applied Surface Science*, 2009, 255: 5669–5673.
- [9] CHU X, CHEN T, ZHANG W, ZHENG B, SHUI H. Investigation on formaldehyde gas sensor with ZnO thick film prepared through microwave heating method [J]. *Sensors and Actuators B: Chemical*, 2009, 142: 49–54.
- [10] CHEN Y W, LIU Y C, LU S X, XU C S, SHAO C L, WANG C, ZHANG J Y, LU Y M, SHEN D Z, FAN X W. Optical properties of ZnO and ZnO: In nanorods assembled by sol-gel method [J]. *The Journal of Chemical Physics*, 2005, 123: 134701.
- [11] ZHANG H, YANG D R, MA X Y, JI Y J, XU J, QUE D L. Synthesis of flower-like ZnO nanostructures by an organic-free hydrothermal process [J]. *Nanotechnology*, 2004, 15: 622.
- [12] FAN H J, LEE W, HAUSCHILD R, ALEXE M, LE RHUN G, SCHOLZ R, DADGAR A, NIELSCH K, KALT H, KROST A, ZACHARIAS M, GÖSELE U. Template-assisted large-scale ordered arrays of ZnO pillars for optical and piezoelectric applications [J]. *Small*, 2006, 2: 561–568.
- [13] CHENG B, SAMULSKI E T. Hydrothermal synthesis of one-dimensional ZnO nanostructures with different aspect ratios [J]. *Chemical Communications*, 2004: 986–987.
- [14] ZHAO X Q, KIM C R, LEE J Y, SHIN C M, HEO J H, LEEM J Y, RYU H, CHANG J H, LEE H C, SON C S, SHIN B C, LEE W J, JUNG W G, TAN S T, ZHAO J L, SUN X W. Effects of thermal annealing temperature and duration on hydrothermally grown ZnO nanorod arrays [J]. *Applied Surface Science*, 2009, 255: 5861–5865.
- [15] ZHAO Q, XU X Y, SONG X F, ZHANG X Z, YU D P, LI C P, GUO L. Enhanced field emission from ZnO nanorods via thermal annealing in oxygen [J]. *Applied Physics Letters*, 2006, 88: 33102.
- [16] WANG H B, WANG H, ZHANG C, YANG F J, YANG C P, GU H S, ZHOU M J, LI Q, JIANG Y. Effect of annealing on the magnetic properties of solution synthesized Zn<sub>1-x</sub>Mn<sub>x</sub>O nanorods [J]. *Materials Chemistry and Physics*, 2009, 113: 884–888.
- [17] LEE J, CHUNG J, LIM S. Improvement of optical properties of post-annealed ZnO nanorods [J]. *Physica E*, 2010, 42: 2143–2146.
- [18] XIANG Q, MENG G, ZHANG Y, XU J, XU P. Chemical Ag nanoparticle embedded-ZnO nanorods synthesized via a photochemical method and its gas-sensing properties [J]. *Sensors and Actuators B*, 2010, 143: 635–640.
- [19] WANG D, SEO H W, TIN C C, BOZACK M J, WILLIAMS J R, PARK M, SATHITSUKSANO H N, CHENG A, TZENG Y H. Effects of postgrowth annealing treatment on the photoluminescence of zinc oxide nanorods [J]. *Journal of Applied Physics*, 2006, 99: 113509.
- [20] LUPAN O, CHAI G, CHOW L. Fabrication of ZnO nanorod-based hydrogen gas nanosensor [J]. *Microelectronics Journal*, 2007, 38: 1211–1216.
- [21] CHEN Z Q, YAMAMOTO S, MAEKAWA M, KAWASUSO A, YUAN X L, SEKIGUCHI T. Postgrowth annealing of defects in ZnO studied by positron annihilation, x-ray diffraction, Rutherford backscattering, cathodoluminescence, and Hall measurements [J]. *Journal of Applied Physics*, 2003, 94: 4807–4812.
- [22] GADZUK J W. Thermally assisted atom transfer on surfaces [J]. *Physical Review B*, 2006, 73: 85401.
- [23] KIM M S, YIM K G, CHOI H Y, CHO M Y, KIM G S, JEON S M, LEE D Y, KIM J S, KIM J S, SON J S, LEE J I, LEEM J Y. Thermal annealing effects of MBE-seed-layers on properties of ZnO nanorods grown by hydrothermal method [J]. *Journal of Crystal Growth*, 2011, 326: 195–199.
- [24] HU Y F, LIU Y, LI W L, GAO M, LIANG X L, LI Q, PENG L M. Observation of a 2D electron gas and the tuning of the electrical conductance of ZnO nanowires by controllable surface band-bending [J]. *Advanced Functional Materials* 2009, 19: 2380–2387.
- [25] SUN S, CHANG X, LI Z. Thermal-treatment effect on the photoluminescence and gas-sensing properties of tungsten oxide nanowires [J]. *Materials Research Bulletin*, 2010, 45(9): 1075–1079.
- [26] DJURIŠIĆ A B, LEUNG Y H. Optical properties of ZnO nanostructures [J]. *Small*, 2006, 2(8–9): 944–961.
- [27] SCHAUB R, WAHLSTRÖM E, RÖNNAU A, LÆGSGAARD E, STENSGAARD I, BESENBAKER F. Oxygen-mediated diffusion of oxygen vacancies on the TiO<sub>2</sub>(110) surface [J]. *Science*, 2003, 299(5605): 377–379.

## 退火处理对氧化锌纳米棒形貌及气敏性能的影响

张建交, 郭二军, 王丽萍, 岳红彦, 曹国剑, 宋 良

哈尔滨理工大学 材料科学与工程学院, 哈尔滨 150040

**摘 要:** 研究水热合成氧化锌纳米棒的高温热稳定性。采用 X 射线衍射和扫描电镜对氧化锌纳米棒的结构与形貌进行表征。采用热重分析研究氧化锌纳米棒在热处理过程中的失重情况。结果表明: 在退火温度低于 400 °C 时, 氧化锌纳米棒具有较好的热稳定性。当退火温度超过 600 °C 时, 氧化锌纳米棒的长径比明显降低并且纳米棒的团聚趋势加剧。退火处理对氧化锌纳米棒的气敏性能具有显著影响。与未经退火处理的氧化锌纳米棒相比, 经历 400 °C 退火处理的氧化锌纳米棒对浓度为  $25 \times 10^{-6}$  的  $H_2$  灵敏度可以从 2.22 提高至 3.56。经历 400 °C 热退火处理的氧化锌纳米棒对  $H_2$  表现出最优的气敏性能。

**关键词:** 氧化锌纳米棒; 退火处理; 气敏性能

(Edited by Chao WANG)